

Anton TURK¹
Jasna PRPIĆ-ORŠIĆ²

Estimation of Extreme Wind Loads on Marine Objects

Review paper

In the structural design of ships and offshore objects wind loads are not usually considered as the key factor in the total loading on those structures, yet the magnitude of the mean static forces and the moments caused by the wind could induce effects in which these forces and moments become critical, provoking cracks and obstructing efficiency during various ship and offshore operations. From a designer's viewpoint, the accuracy of these estimates is important since it influences safety margins, economy of design and operational restrictions.

This paper presents the calculation of stationary wind loads on ships and offshore structures. Wind loads on marine structures, expressed as an ahead force, a side force and the yawing moment, were calculated and compared for four available methods.

Three parameters of a Weibull density distribution function were calculated for a specific location to present an adequate statistical model for describing the extreme wind speed distribution.

Keywords: *wind loads, offshore structures, extreme wind speed*

Procjena ekstremnih opterećenja uslijed djelovanja vjetra na pomorske objekte

Pregledni znanstveni rad

Opterećenja uslijed djelovanja vjetra obično ne predstavljaju najznačajniji čimbenik ukupnog opterećenja konstrukcije. Međutim, srednje statičke sile i momenti uzrokovani vjetrom mogu uzrokovati pojave pri kojima takve sile i momenti postaju kritični zbog pojava pukotina i smanjenja učinkovitosti brodova i pučinskih objekata tijekom izvođenja različitih radnih zadataka. Sa stajališta je projekatnata točnost takvih procjena vrlo važna jer utječe na granicu sigurnosti, ekonomske značajke projekta, te na operativna ograničenja.

U radu je dan je prikaz procjene stacionarnih opterećenja uslijed djelovanja vjetra na brodove i pučinske objekte. Vrijednosti opterećenja uslijed djelovanja vjetra, izražena su kao uzdužna sila, bočna sila i moment zaošijanja, izračunate su i uspoređene za četiri različite postojeće metode.

Kao ilustracija prikladnog statističkog modela, za određenu je lokaciju razdioba ekstremnih brzina vjetra opisana pomoću Weibullove funkcije.

Ključne riječi: *opterećenje uslijed vjetra, pučinski objekti, ekstremna brzina vjetra*

Authors' addresses:

^{1,2} Faculty of Engineering, University of Rijeka

Department of Naval Architecture and Marine Technology Engineering
Vukovarska 58, 51000 Rijeka

¹ e-mail: aturk@rijeka.riteh.hr

² e-mail: jasnapo@rijeka.riteh.hr

Received (Primljeno): 2007-04-20

Accepted (Prihvaćeno): 2008-10-22

Open for discussion (Otvoreno za raspravu): 2010-06-30

1 Introduction

Wind loads on ships constitute a relatively small, yet important part of environmental loads. An accurate knowledge of the magnitude of wind-structure interactions and the resulting load effects, as well as of the character of the wind loads is required for the analyses of propulsion, towing, maneuvering, mooring, stability, deck load capacity, and dynamic positioning. Wind loads on ships and offshore structures have until recently been determined only by model tests, or by statistical methods based on model tests. Wind forces on ships and offshore structures can be more precisely estimated only by the wind tunnel tests. However, the problem is that the wind tunnel tests are quite expensive and time-consuming, so prediction methods described above are often used alternatively.

The magnitude of wind loads on an offshore structure, be it a tension leg platform, a semi-submersible, or a floating production, storage and offloading vessel, can be considerable. Already subjected to wave and current loads below the water, a structure is affected by the wind loads above the water, making such a

structure subject to considerable dynamic loads. In general, wind loadings are most important when platforms are afloat. Wind overturning moments govern hydrostatic stability requirements and wind forces are among major forces which may need to be resisted in the mooring, positioning and towing phases. In this paper, some methods for the prediction of wind forces acting on floating structures [1] as well as the estimation of wind extremes will be presented. One of the most critical features of the design process is the estimation of the worst condition to which a given structure is likely to be exposed in its lifetime, and in particular the prediction of a characteristic value which is associated with a probability of nonexceedance in that time, thus emphasizing the importance of having reliable wind data.

2 Assessment models for wind loads on ships and offshore structures

Information on wind loads exerted on ships and offshore structures is needed when maneuvering, dynamic positioning, stability,

mooring, seaworthiness, and, of course, the notorious sea trials are concerned. In this respect, wind loads exerted on ships have usually been obtained by using empirical/statistical methods or wind tunnel tests. From an aerodynamic viewpoint, vessels and platforms are complex bluff bodies. The wind loads exerted on them are not amenable to theoretical analysis; therefore, empirical calculation procedures or wind tunnel tests carried out on scale models are used to provide estimates of the forces and moments to be expected on full-scale structures. The reason why the wind loads exerted on offshore platforms have been determined by empirical methods or wind tunnel tests is because different layouts of these structures impede a statistical analysis.

Wind loading acting on vessels (Fig. 1) should be determined by appropriate calculation formulas using the drag coefficients C_x , C_y , in the X and Y directions and yaw moment coefficient C_M :

$$R_x = \frac{1}{2} \rho_a U^2 A_T C_x \quad (1)$$

$$R_y = \frac{1}{2} \rho_a U^2 A_L C_y \quad (2)$$

$$M_M = \frac{1}{2} \rho_a U^2 A_L L_{oa} C_M \quad (3)$$

where R_x , R_y and M_M are the components of the wind forces in the X and Y directions and the moment of the wind load about the midship, respectively, ρ_a is the air density and U is the wind velocity. A_T and A_L are the frontal and side projected areas above the water surface and L is the length overall.

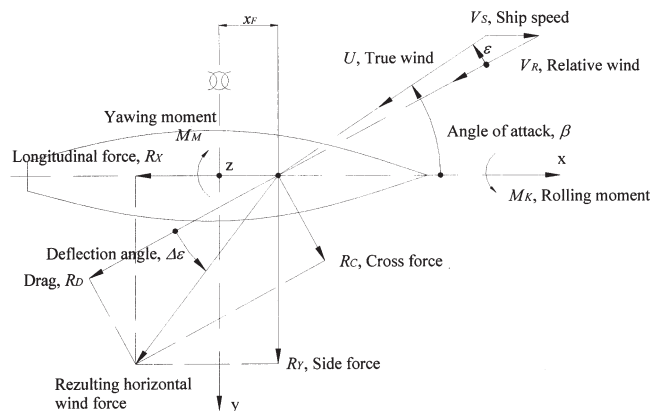


Figure 1 **Coordinates; wind forces and moments**
Slika 1 **Koordinate; sile i momenti uslijed djelovanja vjetrova**

2.1 Wind loads on ships

Hughes [2] investigated wind forces acting on ship superstructures by using models mounted on the underside of a raft towed along a tank at different speeds and at different angles. Based on his experiments, he concluded that for the side wind, the effective area is basically the same as the longitudinal projected area. For the head wind, however, the main hull below the water deck contributes much less than the frontal area of the superstructure with the ratio of approximately 0.3. The wind velocity was determined and the total force acting on a ship was measured. Hughes established an equation for wind resistance as

a function of the wind velocity, wind angle, and the lateral and the transverse projected area of the ship.

$$F = K \rho_a U^2 (A_L \sin^2 \varepsilon + A_T \cos^2 \varepsilon) / \cos(\beta - \varepsilon) \quad (4)$$

where $\beta - \varepsilon$ is the angle difference between the true and the relative wind. For a head wind $\beta = \varepsilon = 0$, the wind resistance becomes

$$R_x = K \rho_a U^2 A_T \quad (5)$$

with K value of approximately 0.6 for all angles ε , varying between 0.5 and 0.65 for different ship types examined. Thus,

$$R_x = 0.734 U^2 A_T \quad (6)$$

Taylor [3] suggested that the air resistance of ordinary ships in a head wind could be assumed equal to that of a flat plate set normal to the direction of motion and having a width B equal to the beam of the ship and a height equal to $B/2$. He derived a resistance coefficient of $C_x = 1.28$ obtained from experiments, so that equation (1) becomes [3]

$$R_x = 1.28 \frac{1}{2} \rho_a U^2 A_T = 1.28 \frac{1}{2} 1.223 \frac{1}{2} B^2 U^2 = 0.783 \frac{1}{2} B^2 U^2 \quad (7)$$

which is similar to Hughes' expression.

Isherwood [4] proposed numerical expressions in the form of coefficients for the lateral and transverse wind forces as well as for the yawing moment, derived from multiple regression analyses of previously published experimental results. Coefficients C_x , C_y , C_M derived from equations (1), (2), (3) are based upon the mean square wind speed U at height z ,

$$U^2 = \frac{1}{h} \int_0^h U^2 dz \quad (8)$$

and h is the height to the top of the superstructure.

The wind coefficients are given by equations, depending on the basic characteristics of the water above the hull. Data were best fitted by using the following forms:

$$C_x = A_0 + A_1 \frac{2A_L}{L^2} + A_2 \frac{2A_T}{B^2} + A_3 \frac{L}{B} + A_4 \frac{S}{L} + A_5 \frac{C}{L} + A_6 M \quad (9)$$

$$C_y = B_0 + B_1 \frac{2A_L}{L^2} + B_2 \frac{2A_T}{B^2} + B_3 \frac{L}{B} + B_4 \frac{S}{L} + B_5 \frac{C}{L} + B_6 \frac{A_{SS}}{A_L} \quad (10)$$

$$C_M = C_0 + C_1 \frac{2A_L}{L^2} + C_2 \frac{2A_T}{B^2} + C_3 \frac{L}{B} + C_4 \frac{S}{L} + C_5 \frac{C}{L} \quad (11)$$

where S represents the length of lateral projection perimeter, C the distance from bow to the centroid of the lateral projected area, A_{SS} the lateral projected area of the superstructure and M the number of distinct groups of masts or king posts. A_0 to A_6 , B_0 to B_6 , and C_0 to C_5 from the above equations are constants presented in a tabular form along with residual standard errors and can be found in [4].

Equations are given to provide the best available means of estimating the above mentioned components of wind force and the wind induced yawing moment and can be applied to a wide range of ship types and configurations and for all angles of the wind relative to the bow. The values predicted from the regression

equations are for the uniform flow which allows the effects of velocity gradient.

Gould [5] presented a numerical procedure to determine the ahead force, side force and yawing moment of most ships in motion or at anchor, in the presence of a natural wind blowing from any direction on the superstructures of ships. The effect of the wind speed over the sea on the effective relative wind speed acting on the ship is argued. Gould determined that for wind profiles over the sea, the surface moves with the wind and the magnitude of the roughness presented by the waves varies with the wind speed. The effects of the wind speed over the sea on the effective relative wind speed affecting the ship were correlated. The author [5] determined that for wind profiles over the sea, the surface moves with the wind and the magnitude of the roughness presented by the waves varies with the wind speed, meaning that the wind speed increment increases the roughness of the sea surface upon which the wind profile over the sea depends. A logarithmic profile is provided as the best approximation for mean wind velocities to the measured wind profiles close to the sea, but it is less representative over the full range of heights of interest when considering forces acting on a ship or oil platform.

Series of model ships were tested in a wind tunnel in uniform and gradient velocity profiles, over a range of wind directions, while uniform wind force coefficients were evaluated for the ahead and the side force [5].

The author [5] simplifies frontal and lateral projections of the superstructure above the required waterline, which are then subdivided into convenient elements recommended as “universal elements” for determining the effective wind speed and the lateral centre of pressure for a vertical gradient of the mean horizontal wind speed. Each of these elements consists of two vertical lines. The wind tunnel data for ships covering a wide range of designs which include variations in the bow shape, the extent of exposed bulwarks, the distribution of lateral area along the length, changes in deck levels, the aspect ratio and the amount of clutter on the upper decks are discussed. Subsequently, possible applications to other ships are given by comparing the listed design which has the most common features to the one under consideration. Furthermore, this data enables the estimation of the forces and moment coefficients for a large variety of ship designs.

The estimation process can be summarized as follows:

- a) Setting power law index (1 / m) for a natural wind profile, $m = \ln(\sqrt{h_1 h_2} / z_0)$ with h_1 and h_2 as the lower and the upper height of interest and z_0 as the roughness length parameter in terms of wind speed.
- b) Choosing reference height and yawing moment centre at x_{ref} / L .
- c) Subdividing frontal and lateral projections into “universal elements” (Fig. 2) and obtaining effective wind speed for gradient wind \bar{U}_x and \bar{U}_y by summarizing throughout each “universal element” to get a reference wind speed and \bar{x}_0 / L which yields \bar{x}_0 as the distance of the lateral centre of pressure from the bow for a beam wind.
- d) For a ship moving at a speed V , \bar{R}_x and \bar{R}_y are evaluated by using equation $\bar{R}^2 = \bar{U}^2 + 2\bar{U}V \cos \phi + V^2$ for appropriate \bar{U}_x and \bar{U}_y , with ϕ being the angle between the plane of natural wind and the longitudinal axis. Subsequently, β_x and β_y are found from the following equation:

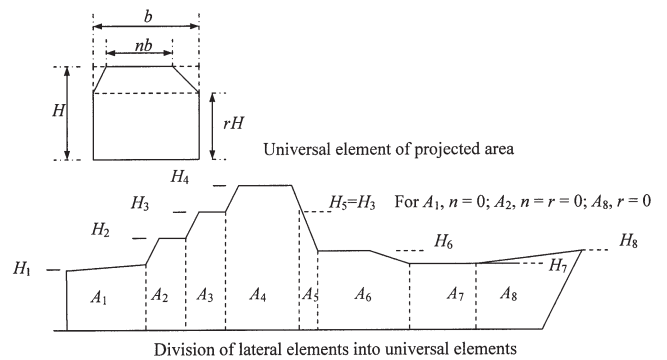


Figure 2 Estimation of velocity area products
Slika 2 Određivanje vjetru izloženih površina

$$\tan\left(\beta - \frac{\phi}{2}\right) = \frac{\bar{U} + V}{\bar{U} - V} \tan \frac{\phi}{2} \quad (12)$$

- e) Using tables (graphs) prepared in the article [5], 15 models are proposed, from which one can be chosen as the closest one to the desired ship characteristics, and by varying wind angles at intervals of 10°, C_x , C_y , and \bar{x} / L are presented in order to obtain components of the wind force and the moment of the wind load about the midship on the superstructure for the considered condition:

$$R_x = \frac{1}{2} \rho_a \bar{R}_x^2 A_T C_x \quad (13)$$

$$R_y = \frac{1}{2} \rho_a \bar{R}_y^2 A_L C_y \quad (14)$$

$$M_M = R_y \left(\bar{x} / L - x_0 / L + x_{ref} / L\right) \quad (15)$$

Blendermann [6], [7], [8], [9], presented a systematic collection of wind load data derived from wind tunnel tests carried out on a scale model. Depending on a random shape of the deck cargo with regard to the kind and distribution, the author suggests that wind loads exerted on ships should be analyzed as statistical data. With that assumption, Blendermann carried out a research that lead to expressions for longitudinal and side force coefficients and coefficients for the yaw and the rolling moments versus the angle of wind attack as a function of the frontal and lateral projected areas:

$$C_x = \frac{R_x}{qA_T}, \quad C_y = \frac{R_y}{qA_L}, \quad C_M = \frac{R_M}{qA_L L}, \quad C_K = \frac{R_K}{qA_L L} \quad (16)$$

where $q = \rho_a / 2U^2$ represents the dynamic pressure of the true wind. Depending on the wind, resulting forces in that respect are the drag R_D and the cross force R_C ; therefore, we can attain the following appropriate drag and cross-force coefficients:

$$C_D = \frac{R_D}{qA_L}, \quad C_L = \frac{R_C}{qA_L} \quad (17)$$

In the analysis, the resulting horizontal force is deflected toward the ship lateral axis and is expressed by a deflection parameter a in connection to deflection coefficient α_0 which is tightly correlated with the maximum longitudinal force coefficient,

$$a = 1 - \frac{\tan \varepsilon}{\tan(\varepsilon + \Delta\varepsilon)} \quad (18)$$

where $\Delta\varepsilon$ represents the deflection angle. The mean deflection parameter \bar{a} as a best fit to experimental data is then presented as a function of the coefficients of the transverse C_{DT} and the lateral C_{DL} resistance of the ship,

$$\bar{a} = 1 - \alpha_0 \frac{C_{DT}}{C_{DL}} \quad (19)$$

The terms yawing-moment lever arm $x_F = LC_M/C_Y$ and rolling-moment lever arm $z_F = H_M C_K/C_Y$ are introduced, with the mean height defined as $H_M = A_L/L$. Thus, four primary wind load parameters are obtained: coefficient of the transverse resistance C_{DT} , coefficient of the lateral resistance C_{DL} , cross-force parameter δ , and rolling-moment factor κ .

Using the classical solution of mathematical flow on the so-called Helmholtz-Kirchoff plate, parametrical loading functions can be expressed as:

$$C_x = -C_{DT} \frac{A_L}{A_T} \frac{\cos \varepsilon}{1 - \frac{\delta}{2} \left(1 - \frac{C_{DT}}{C_{DL}}\right) \sin^2 2\varepsilon}, \quad (20)$$

$$C_y = C_{DL} \frac{\sin \varepsilon}{1 - \frac{\delta}{2} \left(1 - \frac{C_{DT}}{C_{DL}}\right) \sin^2 2\varepsilon}, \quad (21)$$

$$C_M = \left[\frac{s_L}{L} - 0.18 \left(\varepsilon - \frac{\pi}{2} \right) \right] C_Y, \quad (22)$$

$$C_K = \kappa \frac{s_H}{H_M} C_Y, \quad (23)$$

with s_L and s_H as positions of the lateral-plane centroid with respect to the main section, and above the waterline. Reference data C_{DT} , C_{DL} , δ and κ are shown in the tabular form [7].

Numerous experiments and analyses showed that there are only three basic ship shapes with respect to the aerodynamic loading. Based on their parameter characteristics, ships might be classified as multiform shapes (container ships, cargo vessels, fishing vessels, etc.), rectangular cubes (car carriers, ferries, passenger liners, etc.), and longitudinally unsymmetrical shapes (offshore supply vessels, tugs, etc.) The wind loading functions given above do not change and the values of the wind load parameters just have to be matched with an appropriate ship type.

Blendermann's work also involves a prediction on wind loads in extreme winds for floating docks. The air-flow around a dock depends on the incoming wind velocity gradient, and the site settings. Maximum static wind loads usually based on the highest one-minute mean wind speed are calculated. Blendermann also proposed a method for the prediction of wind loads on ships in a non-uniform air flow using experimental data. The non-uniform air flow comes out as a result for an effective dynamic pressure.

OCIMF [10] wind data contain a database of non-dimensional wind force/moment coefficients to be used in the calculation of wind loads on very large crude carriers. In OCIMF report coefficients and procedures for computing wind loads on carriers in the 150,000-500,000 dwt class, with both prismatic and spherical tanks being shown. The wind force and moment coefficients are presented in non-dimensional form for a moored vessel and are applicable to draught conditions ranging from ballasted to fully loaded conditions. For smaller tankers for example, with similar geometry procedures and coefficients are also applicable. The wind coefficients are based upon data obtained from wind tunnel tests conducted at the University of Michigan in the 1960s.

After elaborating several proposed methods for estimating wind loads on ship, an illustration is given showing a comparison between the numerical predictions and experimental results, respectively of the longitudinal force, side force and yaw moment coefficients for the loaded tanker and the tanker in the ballast condition, namely the methods described in [4], [5], [7], and [10].

Based on the review, four methods were selected and implemented in order to carry out a comparative study of the wind loads on ships. The ship selected ship is a tanker with main particulars shown in Table 1.

Table 1 Main particulars of the tanker
Tablica 1 Osnovne značajke tankera

Main particulars of the tanker	Loaded	In ballast
Overall length, m	280.00	280.00
Beam, m	53.50	53.50
Lateral projected area, m ²	2350	5600
Draft, m	14.70	3.80
Height of centre of lateral area above, m	6.83	12.34
Distance of centre of lateral from midship, m	19.30 (forward)	6.44 (forward)
Transverse area, m ²	1025	1750

Figure 3 represents longitudinal force coefficients for the loaded tanker and the tanker in the ballast condition. We can detect some discrepancies within the numerical results, especially concerning the Isherwood method. Even more obvious differences are notable for winds coming from the stern where Isherwood's coefficients tend to overestimate the results as opposed to other three methods, possibly due to the limited range of the experimental results carried out in that study. That suggests that by using Blendermann's, Gould's or the OCIMF method which convey rather good, for the longitudinal force coefficient estimation, we can have sufficiently accurate results and any of these three methods is applicable.

In Figure 4, the side force coefficients are presented. One can observe that there are some differences between the values obtained for the loaded tanker and the tanker in the ballast condition. As for the loaded tanker condition, it can be seen that the side force coefficients for the Gould's method are somewhat overestimated, as opposed to the indicated lower values obtained from Isherwood's method, especially for the angles between 60 and 120 degrees. As for the ballast condition, the results obtained are in agreement for all comparative methods, with the exception of Isherwood's method for wind angles around 90° the results seem to be a bit underestimated. One can agree that, regardless of the ship condition, acceptable methods for determining side force coefficients are Blendermann's method and the OCIMF method.

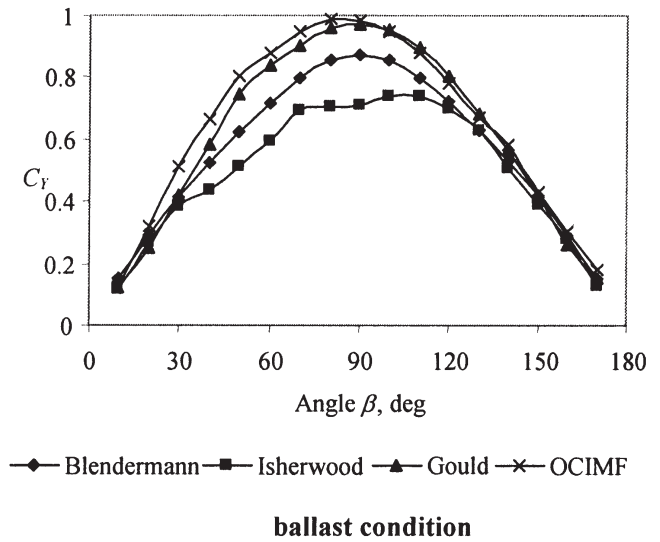
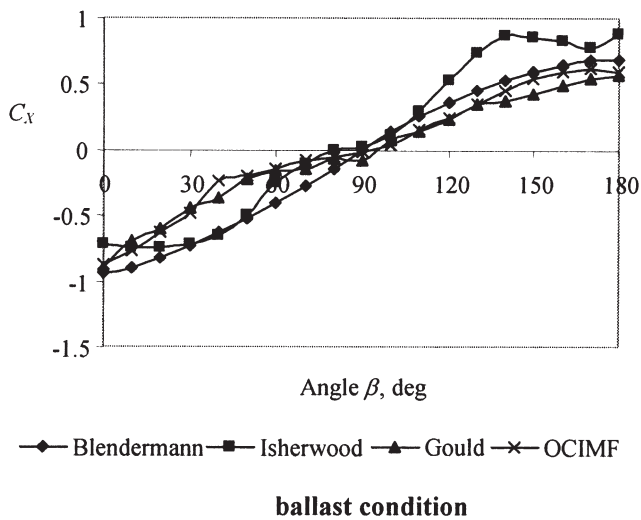
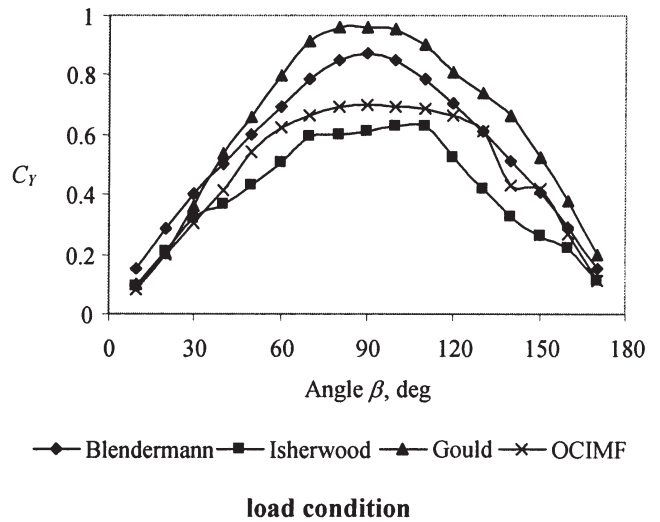
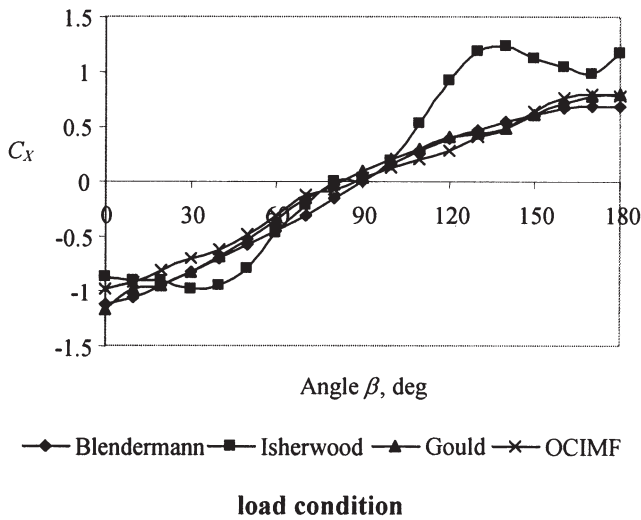


Figure 3 Longitudinal force coefficients, loaded tanker and tanker in ballast
 Slika 3 Koeficijenti uzdužnih sila za tanker pri različitim stanjima krcanja

Figure 4 Side force coefficients, loaded tanker and tanker in ballast
 Slika 4 Koeficijenti poprečnih sila za tanker pri različitim stanjima krcanja

Figure 5 shows the yaw moment coefficients for the loaded tanker and the tanker in ballast. The shapes of these two diagrams are quite different, with the lateral projected area obviously making the difference. As for the loaded tanker, there are qualitative differences between the OCIMF method and the others, with the coefficients derived by the OCIMF method having negative values through the whole range of the wind angle and those derived by the other three displaying a change in sign around wind angles between 50 and 70 degrees. That can be accounted for by the fact that the OCIMF method is developed based on wind tunnel tests carried out solely on very large vessels. This does not necessary imply that the achieved results are incorrect. The values for the yaw moment coefficients for the tanker in the ballast condition are in better agreement, with results being overestimated by Gould's method for wind angles from 0° to 90° and by the OCIMF method for wind angles between 90° and 180°.

Haddara and Soares [11] built a universal model for the estimation of wind loads on ships, using neural network techniques in the parameter identification of the mathematical model with measured input and output data. They did a comparative study between methods already published and Blendermann's experimental data for 19 ships which were used to train the network. In general, the learning time required for learning concepts in the presence of irrelevant features increases proportionally with the data size as well with the number of input layers. Neural network technique does not need any presumption of a functional relationship between variables. Universal mathematical expressions which do not depend on the type of ship were conducted to calculate the coefficients of the wind forces referring to longitudinal and transverse forces and to the yaw moment, respectively.

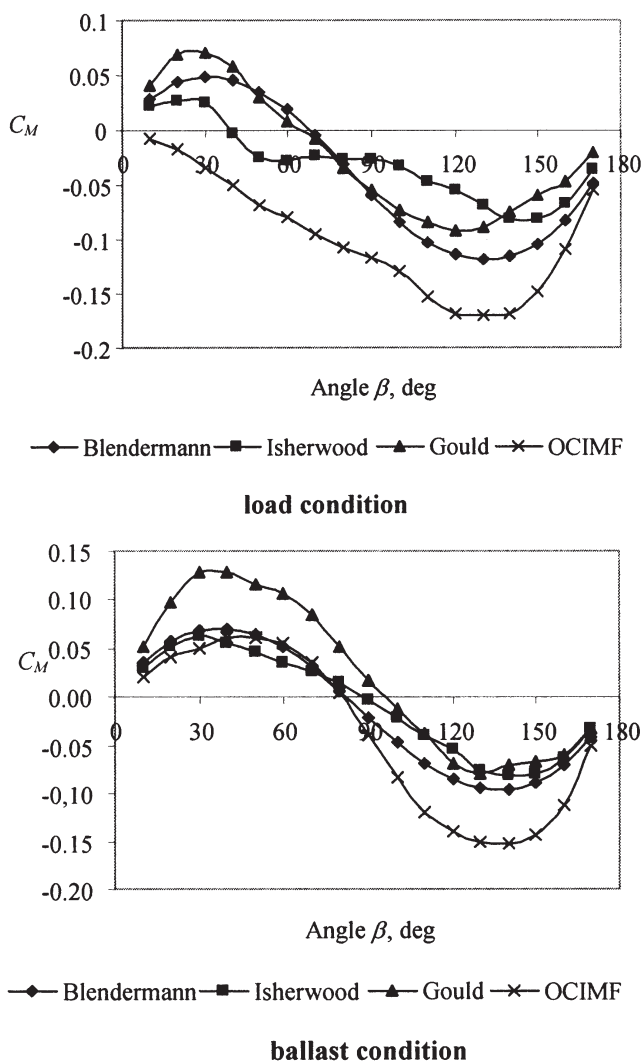


Figure 5 Yaw moment coefficients, loaded tanker and tanker in ballast
 Slika 5 Koeficijenti momenta zaošijanja za tanker pri različitim stanjima krcanja

$$C_k = \sum_{i=1}^m \gamma_{ki} H_{ki} \quad k = 1, 2, 3 \quad (24)$$

where k refers to longitudinal and transverse forces and to the yawing moment.

$$H_{ki} = [1 - e^{-G_{ki}}] / [1 + e^{-G_{ki}}], \quad G_{ki} = \sum_{j=1}^5 w_{kij} x_j \quad k = 1, 2, 3 \quad (25)$$

Input layer had six input features,

$$x_1 = \frac{A_L}{L^2}, \quad x_2 = \frac{A_T}{B^2}, \quad x_3 = \frac{L}{B}, \quad x_4 = \frac{s}{L}, \quad x_5 = \varepsilon, \quad x_6 = 1 \quad (26)$$

where s is the distance between the centre of the A_L and the mid-ship section of the ship. This yields the values for the weights γ_{ki}

and w_{ki} , calculated by the neural network. The obtained results suggest that numerical predictions agree well with experimental ones, which alternatively produce better results than those given by the selected methods.

2.2 Wind loads on offshore structures

Chakrabarti [12] presented a review of present techniques for calculating wind forces on various parts of offshore superstructures. However, because of the obviously complicated geometry and its restrictions, interaction effects must not be neglected. For this reason the wind tunnel test is almost essential.

In addition to mean wind velocity, there are also fluctuating components that have to be taken into account when determining the response of the structure. Usually, there is a large amount of energy in fluctuations which vary in periods from 5 s to 5 minutes and are classified as gusts. Van Karman [13] and Davenport [14] proposed that an in-line velocity fluctuating component should have the following power spectral density:

$$S_{uu}(f) = \frac{4kf\tilde{U}_{10}^2}{(2 + \tilde{f}^2)^{5/6}} \quad (27)$$

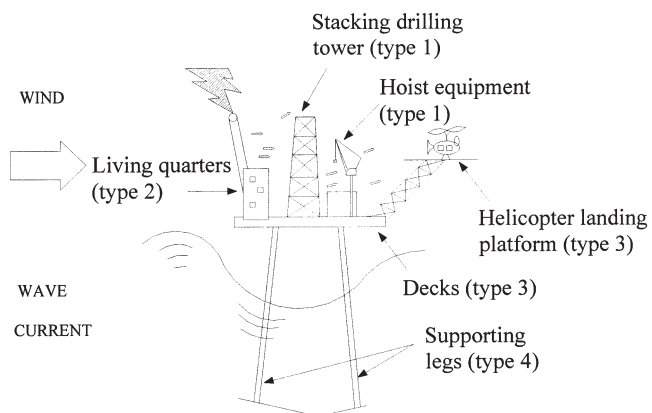
where f is frequency, $\tilde{f} = 1200f / \tilde{U}_{10}$ is normalized frequency, k is surface drag coefficient, and \tilde{U}_{10} is mean wind velocity at the height of 10 m. This is sufficient to calculate wind velocities at any point, but to determine forces on extended areas of the surface, a coherence function linking two points x_1 and x_2 must be introduced and approximated as,

$$\gamma_{x_1x_2}(f) = \exp\left[-\frac{Cfr}{\tilde{U}(z)}\right] \quad (28)$$

where r represents the distance between the points, and C is a coefficient depending on the particular surrounding object.

Figure 6 gives a schema of the layout of the typical oil platform superstructure, with deck structures systemized according to their geometrical type, to determine the mode of response to wind forces [15].

Figure 6 Schematic of wind action on offshore deck structures, showing geometry types
 Slika 6 Djelovanje vjetra na različite dijelove pomorskih konstrukcija



a) Type 1 structures - drilling tower and hoist equipment - consisting of cylindrical members of small diameter. The flow determined by the Reynolds number and the forces calculated by the Morrison equation cause drag because of the relatively low density of the air. Wind pressure at a point can be written as

$$P(t) = 1/2 \rho_a C_D U^2(t) \quad (29)$$

where the drag coefficient C_D depends on the geometrical shape. Pressure can be presented as $P(t) = \bar{P} + p(t)$, and velocity as $U(t) = \bar{U} + u(t)$, consisting of the mean and fluctuating components. By neglecting the terms of order $u(t)$, pressure and velocity spectra are then related as

$$S_{pp}(t) = (C_D \rho_a \bar{U})^2 S_{uu}(f) \quad (30)$$

As with the water flow around a circular cylinder, the airflow may separate, thus giving rise to lift forces.

b) Type 2 structures - living quarters, offices, etc. - usually rectangular surfaces. The flow separates at sharp corners of the objects with the resulting forces on a plane vertical wall facing the wind which are calculated using Davenport's gust factors. The flow separation that occurs may build up lateral forces as well. Equation (29) cannot be applied because it is strictly valid when the dimensions of the obstruction are much smaller than the turbulence wavelength. Therefore, the so-called "aerodynamic admittance function" \mathfrak{K}^2 should be included in the equation (30), which leads to

$$S_{pp}(t) = (C_D \rho_a \bar{U})^2 \mathfrak{K}^2 S_{uu}(f) \quad (31)$$

and $\mathfrak{K} = 1 / \left(1 + \left(2f \sqrt{A / \bar{U}} \right)^{4/3} \right)$, depending on the area of the buildings A , as suggested by Vickery [16]. The next step is to integrate equation (31) over the exposed area for all different points in order to estimate the force spectrum, and, subsequently, to use the coherence function in (28) in order to take the effect of phase variation into account. The generalized pressure spectrum $S_{pp}^r(y_1, y_2, z_1, z_2, f)$ is expressed as a function of two points (y_1, z_1) and (y_2, z_2) in the plane perpendicular to the mean wind direction. This generalized expression leads to a definition of coherence function γ

$$S_{pp}^r(f) = S_{pp}(y_0, z_0, f) A^2 \cdot \iint \gamma(y_1, z_1, y_2, z_2, f) \bullet \bullet \Phi_r(y_1, z_1) \Phi_r(y_2, z_2) \frac{dy_1 dz_1 dy_2 dz_2}{A^2} \quad (32)$$

where $\Phi_r(y, z_1)$ represents the mode shape corresponding to the r^{th} mode, and (y_0, z_0) represent some reference points at which the spectrum $S_{pp}(y_0, z_0)$ is evaluated.

c) Type 3 structures - decks and helicopter landing platform - consisting of flat horizontal surfaces, edge on the wind. The wind flow is in line with surfaces which ultimately correspond to the upward main force trying to lift up this type of the structure. This, however, does not usually occur because of the high stiffness of the elements and the deck plates are made in a rectangular grid fashion which allows the air to pass through, resulting in the pressure equilibrium from both sides.

d) Type 4 structures - platform supporting columns. The main concern here is that during the tow-out the exposed length could be up to 130 m, with a base diameter of 20 m. A full spectral

analysis with certain cross-correlation assumptions must be done since these are basically shell-like structures for which the diffraction theory is not appropriate. Depending on the tapering and the vertical structure of the wind velocity profile, a generalized force spectral analysis is required, as in (32) for rectangular buildings [15]. The surface is, therefore, divided into three independent sets of strips: vertical, front and rear circumferential along with their respective coherence function.

Miller and Davies [17] presented a summary of wind tunnel studies for wind loading on offshore structures after the Norwegian Maritime Institute had conducted a series of wind tunnel studies commissioned by the Department of Energy.

2.3 Classification guides regarding wind phenomena

Det Norske Veritas (DNV) [18] proposes a common reference height of 10 m and a common averaging time of 1 hour for wind velocity changes. Estimation of the average wind speed is given by

$$U(z, t) = U(z_r, t_r) \left(1 + 0.137 \ln \frac{z}{z_r} - 0.047 \frac{t}{t_r} \right) \quad (33)$$

where z represents the height above the still water sea surface and t the averaging time, with z_r and t_r being the reference height and time, respectively. Also, the proposed statistical behaviour of the average wind speed is obtained by the two-parameter Weibull distribution which will be examined in detail in the next section. Gust wind cycles are described by the Harris gust spectrum and deduced by Davenport [14], which corresponds to equation (27).

Wind pressure $q = 1/2 \rho v_{tc}^2$ depends on the air mass density and the wind velocity over a time interval t and at a height z above the mean water level. The wind force F_w on a structural member or a surface acting normal to the member axis or may be calculated as follows:

$$F_w = CqQA \sin \alpha \quad (34)$$

with C as the shape coefficient. Other symbols in (34) have already been elaborated.

Drag forces on cross sections depend upon the shape coefficient, which means that good estimation of the shape coefficient becomes a necessity. Because of the austerity those are given in tables, with appropriately divided definitions taken as for instance, circular cylinders, rectangular cross sections for smooth members and wide objects and for irregular or sphere shaped cross sections. Shape coefficients on three dimensional bodies on horizontal surfaces are also investigated.

In the case of a series of columns, one must take into account the solidity ratio Φ defined as the projected exposed solid area of the frame normal to the direction of the force divided by the area enclosed by the boundary of that frame. However, if two or more parallel frames are located behind each other in the wind direction, the shielding effect may be considered as a shielding factor η with both of those factors proposed in tabular form.

Similarly, ABS [19] treats the calculation of the wind force, F , with the following equation, with C_h representing the height coefficient:

$$F_w = 0.611 U^2 C_h CA \quad (35)$$

Projected area, A , of all exposed surfaces in either the upright or heeled condition is determined in dependence on the shape geometry, e.g. columns, underdecks, clustering of deck houses, isolated houses, structural shapes, cranes, derrick towers, booms and certain types of masts.

Regarding stability criteria, model tests [19] are recommended for the determination of pressures and resulting loads that govern overturning moments on structures of complex shape.

DNV recommends the dynamic analysis of wind sensitive structures to be performed, typically for high towers, flare booms, compliant platforms, such as tension leg platforms and catenary anchored platforms, etc. It is proposed that instantaneous wind force on a wind-exposed structure may be evaluated as a sum of the instantaneous force on every wind-exposed member, giving the instantaneous wind pressure q expressed by the following expression:

$$q = \frac{1}{2} \rho |v_z + u - \dot{x}| (v_z + u - \dot{x}) \tag{36}$$

where u is the gust speed and direction variation, v_z the mean wind speed and direction, and \dot{x} the instantaneous velocity of the structural member. For the purpose of the structural design, the maximum load effect due to the static and dynamic wind can be defined by

$$F_e = F_s + g\sigma(f) \tag{37}$$

with F_s being the static response due to the design average wind speed, $\sigma(f)$ the standard deviation of the dynamic structural responses and g wind response peak factor.

ABS [19] also recommends a direct, nonlinear time domain analysis of dynamic motion responses that should allow the prediction of large amplitude motions and the effects of several nonlinear terms, including the drag force over the instantaneous wetted surface area due to unsteady wind forces. The necessary theoretical information (ABS Average Measured Wind Spectrum) to represent realistic environmental conditions can be categorized by two common scenarios: the extreme wind speed with associated wave height and the extreme wave height with associated wind speed, and can be represented by joint probabilities of wind speed occurrence and wave height.

3 Estimation of wind extremes

A large number of studies have been published that propose the use of a variety of probability density functions to describe wind speed frequency distributions [20]. At present, however, it is the three-parameter Weibull distribution that is the most widely used and accepted in the specialized literature on this subject. The Rayleigh or Weibull probability density functions, are often used in analyses of extreme values at wind speeds and wind energy. It is important to establish the goodness of their suitability for modeling a particular measured distribution. The parameters obtained from the distributions are required to assess the suitability of the functions. Distributional parameters that are commonly used are the parameters of the function itself, such as the parameters of the Weibull function [21]. In the present chapter, the suitability of the Weibull functions is assessed based on a total of 3 parameters (of the probability density and power density distributions). The

Table 2 Sample scatter diagram- winds speed / direction (Area 166, Porcupine, www.meteomer.fr)
 Tablica 2 Dijagram brzina vjetrova za različite smjerove (Područje 166, Porcupine, www.meteomer.fr)

Direction (deg)	0 - 3	3 - 5	5 - 7	7 - 9	9 - 11	11 - 13	13 - 15	15 - 17	17 - 19	19 - 21	21 - 23	>=23	1000
Total													
0 - 15			1	2	3	2	1	1					10
15 - 30			1	2	3	2	2	1					11
30 - 45				2	3	2	2	1	1				11
45 - 60			1	2	2	1	1						7
60 - 75		1	2	2	2	1							8
75 - 90		2	3	3	2	2	1	1	1				15
90 - 105		2	4	2	3	3	1	1					16
105 - 120		1	2	2	2	2	1	1					11
120 - 135		1	2	2	2	2	1	2	1				13
135 - 150		1	1	2	3	3	3	3	1				17
150 - 165		1	4	8	9	8	10	8	6	1			55
165 - 180		1	4	6	10	10	6	4	3	1			45
180 - 195		1	3	7	11	13	9	5	4	1			54
195 - 210		2	4	8	13	18	17	14	9	3			88
210 - 225		2	7	11	14	20	21	13	6	3			97
225 - 240		1	3	7	11	16	15	8	4	1			66
240 - 255		2	4	7	10	10	12	14	9	3	1		72
255 - 270		4	7	10	12	14	18	20	13	3			101
270 - 285		5	10	13	14	15	16	15	9	2			99
285 - 300		3	6	7	8	12	10	10	6				62
300 - 315		1	2	4	10	10	9	6	5	1			48
315 - 330			1	2	6	6	3	3	1	1			23
330 - 345		1	2	4	7	6	3	2	2	1			28
345 - 360			1	3	3	2	1	1	1				12
	23*	32	75	118	163	180	163	134	81	22	1	0	Total

Area: 116
Porcupine

Period
Januray
February
March

Samples >=3 m/s
176611

* Estimated
from the
altimeter

Values expressed
in thousand

Wind speed (m/s)

process of extrapolation plays a fundamental role in this area of analysis and it is essential therefore to fit empirically a convenient probability distribution that describes the available data as closely possible [22].

The 3-parameter Weibull probability distribution can be expressed as

$$F(H_{1/3}) = 1 - \exp \left\{ - \left(\frac{H_{1/3} - \varepsilon}{\theta} \right)^\alpha \right\} \quad (38)$$

where ε represents the location parameter, θ is the scaling parameter and α is the shape parameter. The accuracy of extreme value prediction is significantly affected by the choice of these parameters. If the above expression is rearranged, it may be written as a linear equation

$$\ln(-\ln(1 - F(H_{1/3}))) = \alpha \cdot \ln(H_{1/3} - \varepsilon) - \alpha \cdot \ln \theta \quad (39)$$

where $-\alpha \cdot \ln \theta$ is the intercept α and is the slope.

Having selected one distribution as a likely model, one has to estimate the parameter values that will provide the best empirical fit between the distribution and the data.

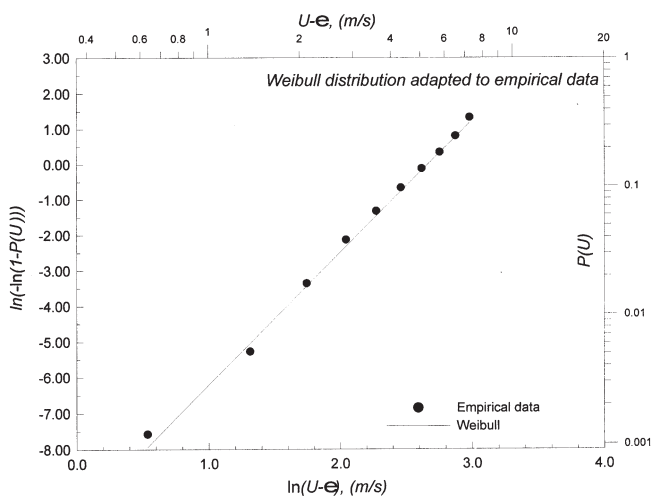
The application of the computational methods is given for the Porcupine area. Table 2 represents the distribution of 176611 collected observations of the wind speeds. The line fitting is presented for the Weibull model in Figure 7, and the resulting CFD curves obtained by the Weibull model are compared with empirical data in Figure 8. Good agreement between them can be noticed.

4 Conclusion

Wind tunnel tests are the most precise means for estimating wind forces on ships and offshore structures. However, these tests are quite expensive, especially in the preliminary design stages of marine objects. Prediction methods described here are, therefore, often used alternatively.

Figure 7 Probability distribution of wind speed for Porcupine region

Slika 7 Razdioba vjerojatnosti brzine vjetera za područje Porcupine



A review of four of the available methods has been given in this paper along with a comparative study carried out between them for the tanker in the loaded and the ballast condition. The wind loads are different for the wind from the port side and from the starboard due to the unsymmetrical arrangement of the working deck. Therefore, the longitudinal force, the side force and the yaw moment coefficients were presented in the range of wind angles from 0° to 180°. For the selected ship, the OCIMF method has proved to be the best, but it is Blendermann's method that can be recommended as the one with the most accurate results. Generally, these two methods are the most comprehensive and reliable among the four selected methods, the reason possibly being that they are the latest methods. The other two are based on the statistical analysis carried out on not too extensive range of experimental work. To conclude, Blendermann's and the OCIMF methods can be used for the wind load estimation of tankers in preliminary stages of the ship design.

A review of present techniques for calculating wind forces acting on various parts of offshore superstructures is also given as well as the DNV and ABS classification guides regarding wind phenomena.

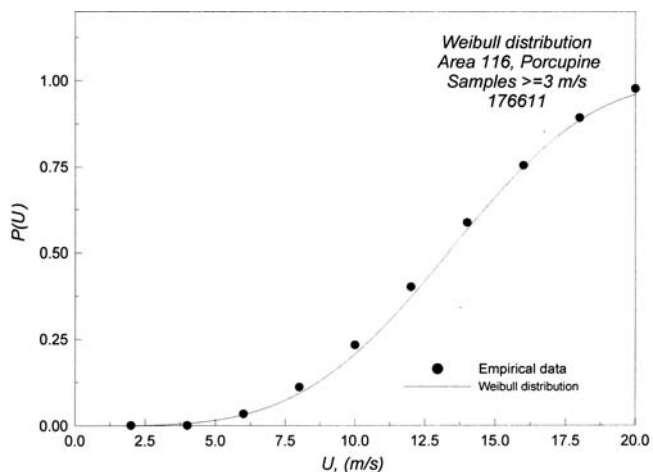
The estimation of the extreme value probability distribution for the assessment of the extreme wind speeds is conducted as well. From the point of view of structural engineering, forecasting the maximum wind speed that is expected to affect a structure during its lifetime is important to the designer.

References

- [1] TURK, A., PRPIĆ-ORŠIĆ, J.: "The Estimation Methods for Wind Loads on Marine Objects", Simpozij Sorta 2006, 499-512, Opatija, 2006.
- [2] HUGHES, G.: "Model experiments on the wind resistance of ships", RINA, Vol. LXXII, 1930.
- [3] TAYLOR, D. W.: "The Speed and Power of Ships. Second Revision", U. S. Government Printing Office, Washington, Original Volume 19 10, 1943.

Figure 8 CFD curves obtained by Weibull model for extremes in Porcupine region (France)

Slika 8 Krivulje kumulativne razdiobe vjerojatnosti prema Weibullovom modelu za ekstreme u području Porcupine (Francuska)



- [4] ISHERWOOD, R. M.: "Wind resistance of merchant ships", *Trans. Roy. Inst. Naval Architects*; 114:327-38, 1972.
- [5] GOULD, R. W. F.: "The estimation of wind loads on ship superstructures", *The Royal Institution of Naval Architects*, monograph, No. 8, p. 34, 1982.
- [6] BLENDERMANN, W.: „Schiffsform und Windlast-Korrelations- und Regressionanalyse von Windkanalmessungen am Modell“, Report No. 533. Institut für Schiffbau der Universität Hamburg, 99 pages plus Appendix. 1993.
- [7] BLENDERMANN, W.: "Parameter identification of wind loads on ships", *J. Wind Enging. Ind. Aerodyn.* 51:339-51. 1994.
- [8] BLENDERMANN, W.: "Estimation of wind loads on ships in wind with a strong gradient", *Proceedings of the 14th International Conference on Offshore Mechanics and Arctic Engineering (OMAE)*, New York: ASME, vl-A, p. 271-7., 1995.
- [9] BLENDERMANN, W.: "Floating docks: prediction of wind loads in extreme winds", *Schiff und Hafen* 48, 4; 67-70, 1996.
- [10] OCIMF. Prediction of wind loads and current loads on VLCCs. 1994.
- [11] HADDARA, M. R., GUEDES SOARES, C.: "Wind loads on marine structures", *Marine Structures*, Volume 12, Issue 3, Pages 199-209, April 1999.
- [12] CHAKRABARTI, SUBRATA K.: "Hydrodynamics of Offshore Structures", *Computational Mechanics Publications*, WIT Press, Southampton, 2001.
- [13] VON KARMAN, T.: "Progress in the Statistical Theory of Turbulence", *Proc. Nat. Acad. Sci.*, Washington, DC, Pages 530-539, 1948.
- [14] DAVENPORT, A. G.: "The application of statistical concepts to the wind loading of structures", *Proc. Inst. Civ. Engrs*, 1961.
- [15] GOMATHINAYAGAM, S., VENDHAN, C. P., SHANMUGASUNDARAM, J.: "Dynamic effects of wind loads on offshore deck structures — A critical evaluation of provisions and practices", *Journal of Wind Engineering and Industrial Aerodynamics*, Volume 84, Issue 3, Pages 345-367, February 2000.
- [16] KAREEM, A.: "Wind induced response analysis of tension leg platform", *J. Struct. Eng. ASCE* 111 (1), 37-55, 1985.
- [17] VICKERY, B. J.: "An Investigation of dynamic wind loads on off shore platforms", OTC 4955, *Proceedings of the Offshore Technical Conference*, Houston, Texas, Pages 527-541, 1985.
- [18] MILLER, B. L., DAVIES, M. E.: "Wind Loading on Offshore Structures – A Summary of Wind Tunnel Studies", *National Maritime Institute*, 1982.
- [19] DNV Classification notes No. 30.5 Environmental conditions and environmental loads, March 2000.
- [20] ABS rules for building and classing. Mobile offshore drilling units, 2008.
- [21] RAMIREZ, P., CARTA, J. A.: "Influence of the data sampling interval in the estimation of the parameters of the Weibull wind speed probability density distribution: a case study", *Energy Conversion and Management* 46, 2419–2438, 2005.
- [22] DORVLO, A.: "Estimating wind speed distribution", *Energy Conversion and Management* 43, 2311–2318, 2002.
- [23] PRPIĆ-ORŠIĆ, J., TURK, A.: "Fitting of extreme wave probability distribution function using genetic algorithm", *Simpozij Sorta, Plitvička jezera*, 2004.